Atomic force microscope manipulation of Ag atom on the Si(111) surface

Batnyam Enkhtaivan and Atsushi Oshiyama
Department of Applied Physics, The University of Tokyo, Hongo, Tokyo 113-8656, Japan
(Received 27 September 2016; revised manuscript received 15 December 2016; published 30 January 2017)

We present first-principles total-energy electronic-structure calculations that provide the microscopic mechanism of Ag atom diffusion between the half unit cells (HUCs) on the Si(111)-(7×7) surface with and without the tip of the atomic force microscope (AFM). We find that, without the presence of the AFM tip, there are three pathways of inter-HUC diffusion. The pathway, in which the diffusing atom passes over the nanohole of the surface, has the lowest energy barrier. The diffusion along this pathway between the two HUCs is almost symmetric with the energy barrier of about 0.8 eV in both directions. In the other two pathways, the adatom diffuses along the edge of the nanohole. The diffusion along these two pathways have an energy barrier of about 1 eV. With the presence of the tip, we find that the reaction pathways are essentially the same, but the diffusion along the edge of the nanohole has a lower energy barrier than the diffusion over the nanohole. Thus the diffusion channel is changed by the presence of the tip. In the diffusion along the edge of the nanohole, the energy barrier in one direction is substantially reduced to be 0.2–0.4 eV by the tip, while that of the diffusion in the reverse direction remains larger than 1 eV. The Si tip reduces the energy barrier more than the Pt tip due to the flexibility of the tip apex structure. In addition to the reduction of the barrier, the tip traps the diffusing adatom preventing diffusion in the reverse direction. Also we find that the shape of the tip apex structure is important for the adatom's trapping ability. The bond formation between the AFM tip atom and the surface adatom is essential for atom manipulation using the AFM tip. Our results show that atom manipulation is possible with both the metallic and semiconducting AFM tips.

DOI: 10.1103/PhysRevB.95.035309

I. INTRODUCTION

Atom-scale resolved structural images of solid surfaces have been achieved by the scanning tunneling microscope (STM) [1] and the atomic force microscope (AFM) [2] by measuring the tunneling electric current between the probing tip and the surface, and the force acting on the probing tip, respectively. Apart from the surface imaging, these scanning probe techniques have also been utilized for manipulating atoms on surfaces. Eigler and Schweizer demonstrated the first atom manipulation by creating the IBM company logo with a Xe atom on a Ni surface by laterally moving the atoms by the STM [3]. In the following year, Lyo and Avouris reported removal and deposition of a single Si atom on a Si surface, showing the possibility of the vertical manipulation also using the STM [4]. A decade later, Oyabu *et al.,* reported atom manipulations on Si surfaces by the AFM [5], expanding the feasibility of atom manipulation to nonconductive surfaces.

Since then, many types of atom manipulation by the AFM probe have been achieved. They include vertical interchange of the tip and surface atoms on the Sn-covered Si(111) surface [6], lateral interchange of adatoms on the Ge(111) [7] and on the Si(111)[8] surfaces, and lateral manipulation of single Si and Ge adatoms on the Si(111) [9,10] and the Ge(111) [11] surfaces, respectively.

Recently, Sugimoto *et al.* succeeded in realizeing a new manipulation scheme named "gate control" in which the diffusion of Ag, Au, Pb, Sn, and Si atoms on the Si(111)-(7×7) surface is enhanced by placing the Pt-Ir coated Si tip above the surface [12]. It has been observed that the adatoms on the Si(111)-(7×7) surface frequently diffuses in the surface half unit cell (HUC), while the inter-HUC diffusion is hindered by a high potential energy barrier. The experimentally observed inter-HUC diffusion barrier of an Ag adatom is more than 0.8 eV [13,14]. Sugimoto *et al.* induced the inter-HUC diffusion of the adatom by placing the AFM/STM [15] or AFM tip at a certain position slightly off the boundary of HUCs. By analyzing the tunneling current and the frequency shift of the cantilever measured simultaneously, they concluded that diffusion control is purely due to the chemical interaction between the tip and the diffusing atom, being neither due to the electric field nor mechanical contact between the tip and the surface. In this sense, this gate control is a different phenomenon from the direct manipulation by the mechanically contacted probe discussed in the past [16,17]. Sugimoto *et al.* also performed the controlling of Sn diffusion on the Si(111) surface by the Si AFM tip. This opened exciting possibilities of the fabrication of atom-number determined nanoclusters on the surface [18–20]. However, albeit the experimental demonstrations, the microscopic mechanisms of the gate control is totally unknown.

The growth of silver on the Si(111) surface has been the focus of many studies [21–24], because of the low intermixing between the two substances. Also, many studies in both experiment and theory regarding the state of the single Ag atom on the Si(111)-(7×7) have been done [13,14,25–29]. The theoretical works have concentrated on clarification of the stable positions and diffusion pathway inside the HUC [29,30]. Wang *et. al.* presented the static potential energy surface (PES) of a single Ag atom on the Si(111) surface, and gave clear understanding of the typical STM images [30].

Therefore, to clarify the microscopic mechanism of the diffusion control of an adatom by the tip of the scanning probe microscope, we choose the system in which Ag atom was adsorbed on the Si(111) substrate as a representative system and have performed extensive density-functional calculations. We first obtain the PES of the Ag atom confirming the result of previous work [30] and examine the inter-HUC diffusion

without the AFM tip. We have identified three diffusion pathways. The corresponding energy barriers are calculated. We then examine the modification of the diffusion process by placing the Si and the Pt tips at a certain position, exploring diffusion pathways, and calculating the diffusion barriers. This is reasonable since the frequency of the tip oscillation (order of kHz) is much lower than the time scale of atomic motion (order of THz). We find that the presence of the tip lowers the diffusion barrier and enhances the inter-HUC diffusion. The extent of the modification significantly varies depending on the flexibility of the tip apex structure.

The paper is organized as follows. The calculational methods and the pertinent conditions for the calculations are explained in Sec. II. The inter-HUC diffusion of the Ag atom without the AFM tip is described in Sec. III A. In Secs. III B 1 and III B 2 the modification of the adatom diffusion process by the Si and the Pt tips is described, respectively. Finally, we summarize our findings in Sec. IV.

II. CALCULATIONS

Calculations are performed within the framework of the density functional theory (DFT) [31,32] using the Vienna *ab initio* simulation package (VASP) [33,34]. The generalized gradient approximation (GGA) [35] is used for the calculation of the exchange-correlation energy. Projector augmented-wave (PAW) potentials [36,37] are adopted to describe the electron-ion interaction. We use the cutoff energy of 250 eV for the plane-wave basis.

Each substrate surface is simulated by a repeating slab model. When the AFM tip is included, the atomic slab is separated from its adjacent image slabs by the vacuum region so that the atomic distances between the different slabs are more than 6 Å, which is found to be large enough to neglect the interaction between the slab and its images [38]. Without the AFM tip, the slabs are separated by more than 8 Å distance. The slab for the Si(111)-(7×7) surfaces is simulated by six atomic layers in addition to the adatom layer. The atoms at the bottommost layer of the slab are terminated with H atoms to remove unsuitable dangling bonds electronically. In the lateral directions, the Si(111)-(7×7) surface is simulated by the dimer-adatom-stacking-fault (DAS) model of Takayanagi *et al.* [39]. Only Γ point is sampled for the Brillouin zone integration since the supercell cells are large. Structural optimization is performed using calculated Hellmann-Feynman forces. All the atoms except for the bottommost layer atoms and the attached H atoms are relaxed until the forces acting on the atoms are smaller than 0.1 eV/Å. The conditions explained above assure that the numerical error of the binding energy of the Ag atom is less than 5 meV. The binding energy is the total energy difference of the isolated Ag atom and the isolated surface from the combined system of the Ag atom and the surface.

The PES is obtained by calculating the binding energy of the Ag atom at the grid points of 64 × 64 rectangular grids in the rectangular unit cell of the Si(111)-c(7×7) surface and by interpolating the values between the grid points with Fourier transformation. In these calculations, the (x, y) coordinates of the Ag atom are fixed.

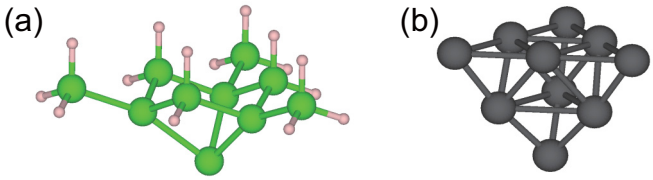

FIG. 1. The model of the (a) Si and (b) Pt tips considered in the calculation. The green (medium), purple (small), and black (large) spheres depict Si, H, and Pt atoms, respectively.

To identify the reaction pathways of the diffusing atom and the corresponding energy barriers, we adopt the climbing-image nudged elastic band (CINEB) method [40]. This method provides the saddle point energy, while partly assuring the continuity of the reaction pathway compared with the hyperplane constraint method [41], by introducing fictitious elastic forces during the energy minimization. In each barrier calculation of an elementary reaction, three image configurations are considered between the initial and the final states. In the whole reaction, there are several metastable configurations. We determine the reaction pathway between the two metastable, i.e., the initial and the final, configurations. In actual calculations, we first explore the metastable configurations and then search for the reaction pathways. When the tip is absent, the metastable configurations are determined from the calculated PES. When the tip is introduced to the system, the metastable configurations are explored in the vicinity of the previously obtained ones by the structural relaxation. The entropy term in the free-energy barrier is not considered in the present calculation by assuming that the difference in the vibrational spectrum between the (meta)stable and transition states plays a minor role.

We consider semiconductor and metallic AFM tips composed of Si and Pt atoms, respectively. The Pt tip is utilized as a simple version of the Pt-Ir coated tip used in the experiment [12]. The tips are simulated by the atomistic model shown in Fig. 1. The Si tip model consists of 10 Si atoms and 15 H atoms. This model is used in previous works [9,10,38,42–46]. The Pt tip model consists of ten Pt atoms. In our calculations, we have done structural minimization of these tips along with the surface atomic configurations. The H atoms and the Si atoms bonding with the H atoms in the Si tip, and the Pt atoms at the far side from the surface in the Pt tip, however, are fixed during the geometry optimization.

The force acting on the AFM tip is obtained by summing force acting along the z direction on the fixed atoms of the tip.

III. RESULTS

A. Adatom diffusion without the AFM tip

The calculated PES of the Ag atom on the Si(111)-(7×7) surface is shown in Fig. 2(a). There are three potential energy wells, the areas in blue color, in each basin [47] and the depths of the potential wells are asymmetric between the HUCs. The distinct (meta)stable adsorption sites are labeled as F_1 and F_2 in the faulted-HUC (FHUC), and U_1 and U_2 in the unfaulted-HUC (UHUC) [see Fig. 2(b)]. The U_1, U_2, and F_2 sites have the binding energy of about 2.30 eV, and the F_1 site has about

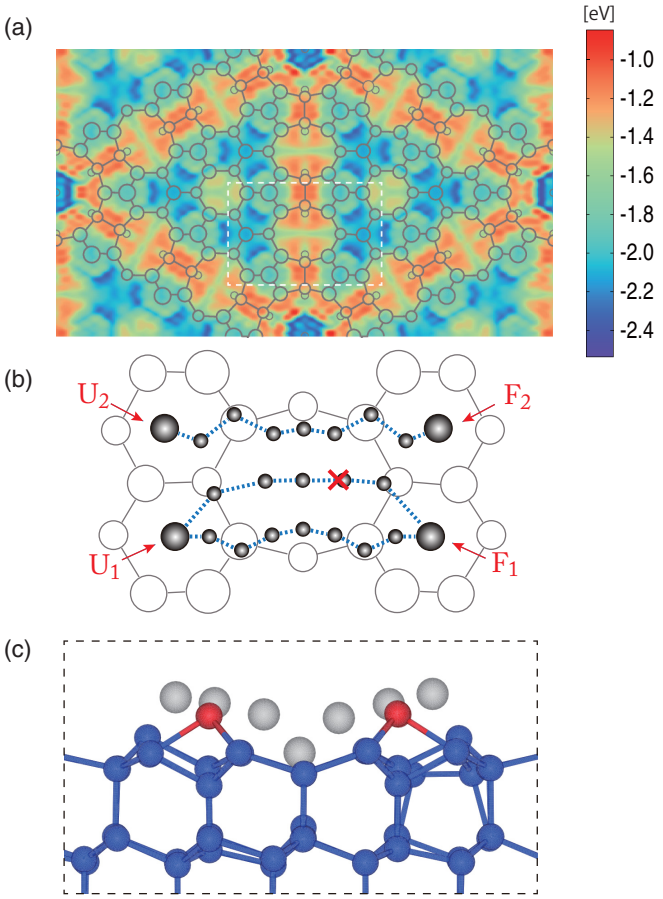

FIG. 2. (a) The calculated potential energy surface (PES) of an Ag adatom on the Si(111)-(7×7) surface as well as the schematic top view of the surface structure. (b) The atomic trajectories in the adatom diffusion pathways. (c) The side view of the atomic configurations of *pathway 3*. In (a), the blue color shows large binding energy and the red color shows smaller binding energy. In the schematic structure, the size of the circle is smaller for the lower layer atoms of the substrate. In (b), the enlarged view of the surface region surrounded by a white rectangle in (a) is shown. The distinct stable and metastable positions of Ag atom are labeled as U_1 and U_2 in the UHUC, and F_1 and F_2 in the FHUC. The diffusion pathways between these positions are shown by the blue dashed lines. The small gray circles on the pathways depict the position of the Ag atom in the image configurations of CINEB calculations. The red x mark shows the lateral position of the tip apex atom of the AFM tip. In (c), the red and blue balls depict the Si adatoms and the Si atoms of the lower layers of the surface, respectively. The silver balls show the positions of the Ag atom in the image configurations of CINEB calculations along *pathway 3*.

a 30 meV larger binding energy than the others. These results are in agreement with the previous works [29,30].

From the PES, it is expected that the diffusion between the HUCs occurs through three channels, i.e., between U_1 and F_1 (*pathway 1*), between U_2 and F_2 (*pathway 2*), and through the potential valley between them (*pathway 3*). The pathways obtained by our CINEB calculations are shown by blue dashed lines in Fig. 2(b). The obtained energy profiles along them are shown in Fig. 3. There are metastable configurations right in the middle of *pathway 1* and *pathway 2*, each labeled as M_1 and M_2, respectively. The energy barriers of $U_1 \rightarrow M_1$

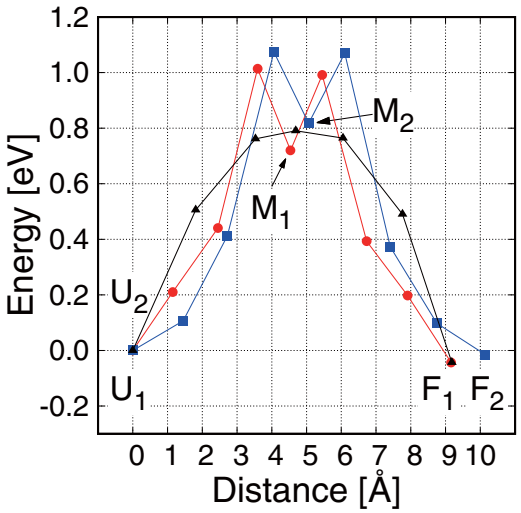

FIG. 3. The energy profiles of the Ag adatom diffusion along *pathway 1* (red circle), *pathway 2* (blue square), and *pathway 3* (black triangle) without the AFM tip. The abscissa is the distance between Ag atoms in the NEB image configurations and the initial structure. The ordinate is the total energy difference of the NEB image configurations from the initial structure.

and $M_1 \rightarrow F_1$ processes are 1.01 and 0.27 eV, respectively, and those of the reverse $F_1 \rightarrow M_1$ and $M_1 \rightarrow U_1$ processes are 1.03 and 0.29 eV, respectively. *Pathway 3* has the lowest energy barrier of 0.79 eV in $U_1 \rightarrow F_1$ direction. The high energy barriers for the diffusion in either direction between the HUCs show that the inter-HUC diffusion is an infrequent event at room temperature. There is a slight asymmetry in the diffusion along *pathway 1* (see Fig. 3). Contrary to this, the diffusion along *pathway 2* is almost symmetric, having diffusion barriers of 1.07 and 0.25 eV for the $U_2 \rightarrow M_2 \rightarrow F_2$ process, and 1.08 and 0.26 eV for the $F_2 \rightarrow M_2 \rightarrow U_2$ process. The experimentally observed energy barriers of $F_1 \rightarrow U_1$ and $U_1 \rightarrow F_1$ processes are about 0.81 and 0.9 eV, respectively [13,14]. The calculated diffusion barriers along the three pathways are comparable to each other but the lowest barrier 0.79 eV emerges along *pathway 3*. This value is in good agreement with the experimental values, showing that *pathway 3* is the dominant path for the inter-HUC diffusion.

Regarding the atomic configuration, we find that the Ag atom in the saddle point configuration of *pathway 3* is located at the same height as the second layer Si atoms of the surface. This is due to the absence of the lower layer Si atoms, forming a nanohole below the Ag atom at the saddle point [see Fig. 2(c)].

B. Ag atom diffusion with the AFM tip

In this section we show the modifications of the diffusion barriers and pathways by the AFM tips (Si and Pt tips). We have considered the cases in which the tip-surface distances are 3.5, 4.0, 4.5, and 5.0 Å. The tip-surface distance is defined as the distance between the tip apex atom and the surface adatom of the Si(111) surface before structural relaxation. For simplicity we focus on the UHUC → FHUC diffusion of the Ag atom. The AFM tip is placed at the red x mark

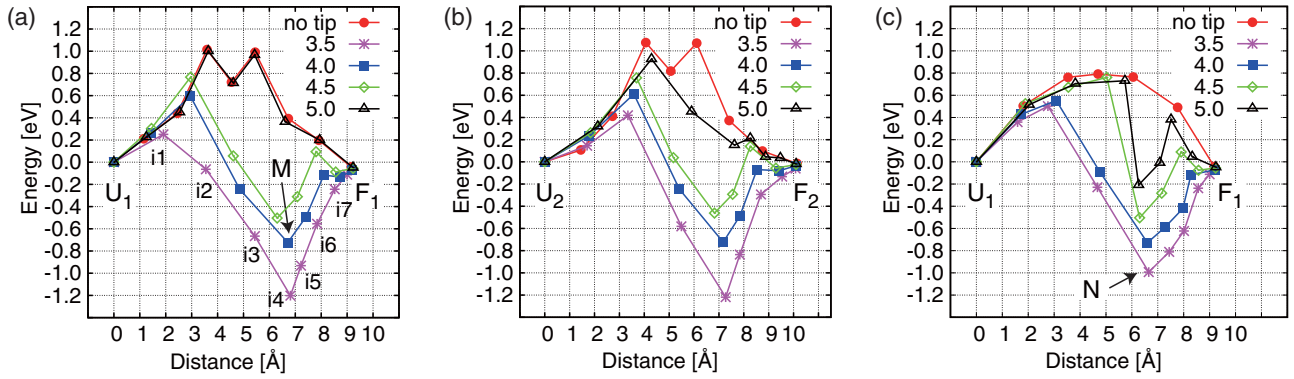

FIG. 4. The energy profiles of the Ag adatom diffusion between the HUCs on the Si(111) surface. (a), (b), and (c) Energy profiles along *pathway 1*, *pathway 2*, and *pathway 3* with the four tip-surface distances are shown, respectively. The circle (red line) is the energy profile of the Ag atom diffusion without the presence of the AFM tip. The triangle (black line), the diamond (green line), the square (blue line), and the asterisk (magenta line) are the energy profiles of the diffusion when the tip-surface distances are 5.0, 4.5, 4.0, and 3.5 Å, respectively. The labels and the axes are the same as those in Fig. 3. In (a), the intermediate states between U_1 and F_1 in the case of the tip-surface distance of 3.5 Å are labeled by i1 ∼ i7.

as shown in Fig. 2, corresponding to the tip position in the experiment [12].

1. *The effect of the Si tip on the diffusion*

The diffusion pathways are essentially the same as those of the Ag atom diffusion without the presence of the tip. The energy profiles along *pathway 1*, *pathway 2*, and *pathway 3* with the presence of the Si AFM tip are shown in Figs. 4(a), 4(b), and 4(c), respectively. First, let us describe the diffusion along *pathway 1*. When the tip-surface distance is 5 Å, the energy profile is not modified and is the same as that of the Ag atom diffusion without the AFM tip. However, as the tip further approaches the surface, it is substantially modified. It becomes significantly asymmetric showing that the FHUC → UHUC diffusion is less probable than the intended UHUC → FHUC diffusion of the Ag atom. There are two kinds of modifications in the energy profile, namely the reduction in the rate determining diffusion barrier and the appearance of local energy minimum. When the tip-surface distance is 4.5 Å, the barrier height decreases from 1.01 to 0.77 eV. With the further approach of the tip to the distances of 4.0 and 3.5 Å, the barrier height becomes 0.60 and 0.25 eV, respectively. The reduced diffusion barrier indicates that the inter-HUC diffusion is enhanced by the presence of the AFM tip. Unlike the UHUC → HUC diffusion, the energy barrier for the diffusion in the reverse direction remains larger than 1 eV at any tip-surface distance, hindering the unintended reverse diffusion to take place. This finding explains the one-way character of the adatom diffusion observed in the experiment [12]. The drastic decrease of the diffusion barrier is due to the flexibility of the tip apex structure of the Si tip [48]. We explain the situation in detail in the case of the tip-surface distance of 3.5 Å. The tip apex atom shifts downward by 0.44 Å in the i1 configuration [see Fig. 4(a)], stretching the backbonds from 2.47 (before structural relaxation) to about 2.64 Å. The distance between the tip apex atom and the Ag atom is 4.87 Å. The tip apex atom further moves toward the Ag atom in i2 configuration and the three backbonds become 2.50, 2.68, and 3.22 Å (0.86 Å from its rest position). Therefore, the tip reduces the energy barrier of the diffusion from a large distance. The importance of the flexibility of the tip apex structure in atom manipulation has been found from our previous work [38]. The current finding is a corroboration of such a general statement.

The dip (or the local energy minimum) in the energy profile also deepens as the tip-surface distance becomes small. The large dip in the energy profile shows that the Ag atom is trapped by the AFM tip proving the picture provided by the experimenters correct [12]. However, in the configuration corresponding to the energy dip, the Ag atom is not right under the tip apex atom. Rather, it is bonding with multiple Si atoms in agreement with the previous study that stated the preference of an Ag atom for the multicoordination with the Si atoms [29]. As an example, the atomic structure of the *M* configuration [see Fig. 4(a)] is shown in Fig. 5(a). The Ag atom is bonding with three Si atoms: tip apex atom, Si adatom (red ball), and Si atom in lower layer. The bond length between the Si adatom and the lower layer Si atom, bonding with the Ag atom, is stretched from 2.47 to 2.68 Å. When the AFM tip approaches further, the Ag atom starts to interact with the second layer Si atoms of the tip. In the i4 configuration with the tip-surface distance of 3.5 Å, the Ag atom bonds with four Si atoms: two Si atoms of the tip and two Si atoms of the surface.

The modifications of the energy profile of the diffusion along *pathway 2* are essentially the same as those of *pathway 1*. The barrier heights become 0.93, 0.76, 0.61, and 0.42 eV when the tip-surface distances are 5.0, 4.5, 4.0, and 3.5 Å, respectively. The Ag atom is also trapped by the tip when the tip-surface distance is small enough. The atomic configurations of the trapped states are similar to those of *pathway 1*, in which the Ag atom bonds with three or four Si atoms. Such modifications are due to the bond formation between the tip apex atom and the Ag atom. It is confirmed by the charge density distribution analysis [see Fig. 5(b)]. The analysis shows that the charge is redistributed and accumulates in the intermediate region between the Ag atom and the tip apex Si atom when the distance between them is short. Moreover, it can be seen that the bonds between the tip atoms including the second layer atoms and the Ag atom are formed, and at the same time the bonds between the apex and the second-layer atoms are weakened.

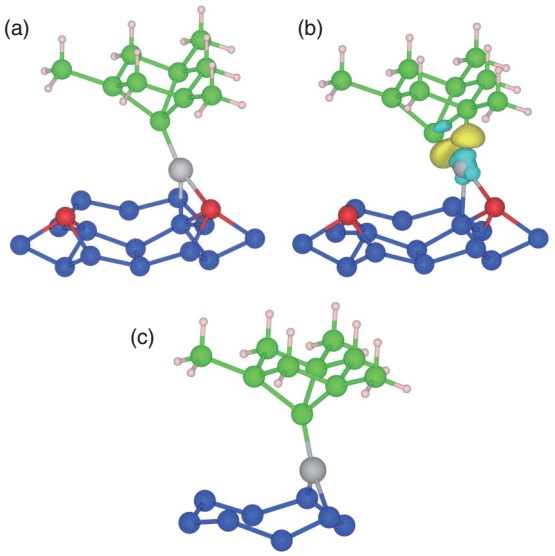

FIG. 5. The atomic structure of the *M* configuration (a), the charge density redistribution between the tip and surface in the i4 configuration (b) shown in Fig. 4(a), and the atomic structure of the *N* configuration (c) shown in Fig. 4(c). The green, yellow balls are tip Si and H atoms, respectively. The silver ball depicts the Ag atom. The red and blue balls are Si adatoms and Si atoms of the lower layers of the surface, respectively. In (b), the yellow and blue regions depict the charge density increase and decrease, respectively.

The energy profiles of the diffusion along *pathway 1* and *pathway 2* when the tip-surface distance is 5.0 Å are significantly different. The energy profile of the diffusion along *pathway 2* becomes asymmetric, while that of the diffusion along *pathway 1* remains almost unchanged by the tip. It is due to the nature of the interaction between the tip apex atom and the Ag atom. To get an insight to this, we consider a simple case in which the Si tip approaches the Ag atom adsorbed at U_1 site from above. The Ag atom is at the site U_1 for it is the most stable adsorption site in the HUC. The obtained force acting on the tip and the change in the total energy of the system with the decreasing distance between the tip apex and Ag atom are shown in Fig. 6. As shown in the force-distance curve of the Si tip placed over the Ag atom, at around 5.0 Å, a slight change in the distance between the tip apex atom and the Ag atom results in a sudden increase in the force acting on the AFM tip. Therefore, the difference in the energy profiles shows that the Ag atom in *pathway 2* diffuses closer to the tip apex atom than the Ag atom in *pathway 1*.

The modifications of the energy profile of the diffusion along *pathway 3* are different from those of *pathway 1* and *pathway 2*. When the tip-surface distances are 4.5 and 5.0 Å, the energy barrier is not reduced. This is due to the large distance between the Ag atom and the tip apex atom compared to that in *pathway 1* and *pathway 2*. As mentioned in Sec. III A, in *pathway 3*, the Ag atom is lowered to the same height as the second layer atoms of the substrate. As the tip approaches the surface to 4.0 Å, the energy barrier and the depth of the trap potential becomes similar to those of *pathway 1* and *pathway 2*. However, at the tip-surface distance of 3.5 Å, the depth of the trap potential is shallower than those of the other two pathways.

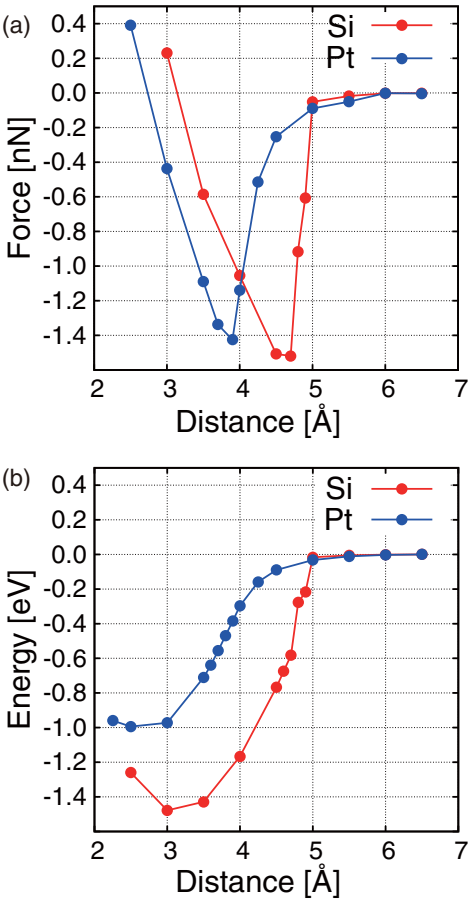

FIG. 6. (a) Force-distance and (b) energy-distance curves of Si and Pt tips over the Ag atom on the Si(111) surface. The abscissa is the distance between the tip apex atom and the Ag atom on the Si surface before structural relaxation. The blue and red lines correspond to the Si and Pt tip results, respectively. The negative values of the force and the energy mean the attractive force on the tip and the energy gain, respectively.

As shown in Fig. 5(c), at the trapped state [*N* configuration shown in Fig. 4(c)], the Ag atom interacts only with the tip apex atom, unlike the trapped states of *pathway 1* and *pathway 2*.

The above results indicate that the dominant diffusion channel for the adatom changes from *pathway 3* to *pathway 1* and *pathway 2* during the atom manipulation utilizing the Si tip.

2. *The effect of the Pt tip on the diffusion*

Here we present the modifications by the Pt tip of the diffusion of the Ag atom on the Si(111) surface. The energy profiles of the Ag atom diffusion from U_1 to F_1 along *pathway 1* and *pathway 3* with different tip-surface distances are shown in Fig. 7. First, we describe the diffusion along *pathway 1*. With the shorter tip-surface distance, the energy barrier of the Ag atom diffusion is reduced and the energy profile becomes asymmetric with the appearance of the local energy minimum. However, as it can be seen, the Pt tip does not decrease the energy barrier as drastically as the Si tip. With the tip-surface distances of 5.0, 4.5, 4.0, and 3.5 Å, the energy barrier of the rate determining process becomes 0.97, 0.92, 0.72, and

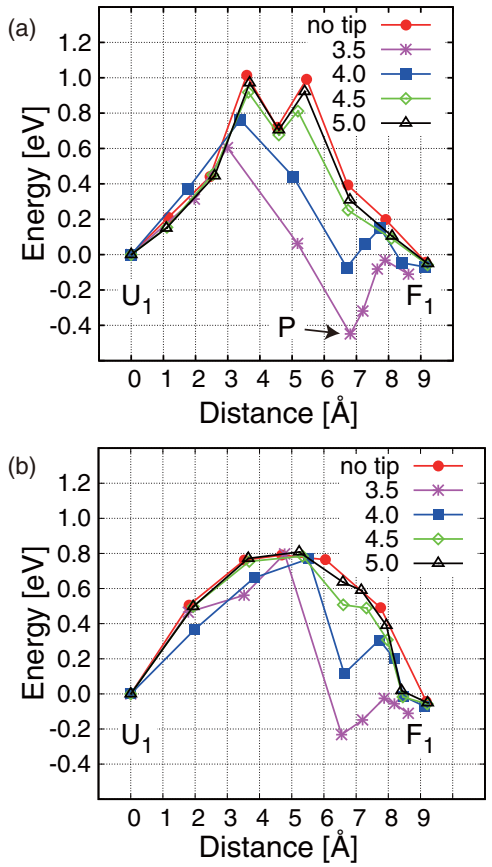

FIG. 7. The energy profiles of the Ag atom diffusion with the presence of the Pt tip. In (a) and (b), the energy profiles along *pathway 1* and *pathway 3* are shown, respectively. The labels and the axes are the same as those in Fig. 4.

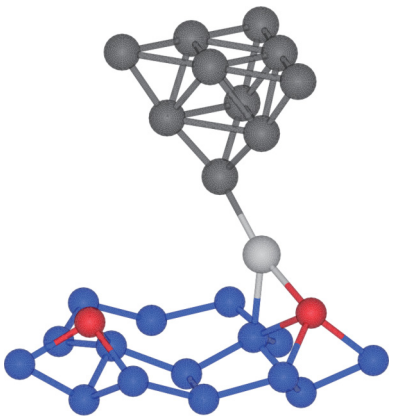

FIG. 8. The atomic structure of the *P* configuration shown in Fig. 7(a). The black and silver balls depict the Pt and the Ag atoms, respectively. The red and blue balls depict the Si adatoms and the lower layer Si atoms of the surface, respectively.

0.60 eV, respectively. These energy barriers are significantly higher than the energy barriers modified by the Si tip. This difference between the Si and Pt tips are due to the difference in the flexibility of the tip apex structure. Unlike the Si tip, the tip apex atom of the Pt tip does not move much to create a bond with the Ag atom. During the diffusion, the Pt atom shifts 0.19 Å at most from its unrelaxed position when the tip surface distance is 3.5 Å. The force-distance curve and the change in the total energy of the system, in which Pt tip approaches the Ag atom from above, are shown in Fig. 6. Considering that the maximum attractive forces acting on the Si and Pt tips are almost the same when the tip is interacting with the Ag atom on the Si surface [see Fig. 6(a)] and the difference in the shift of the tip apex atoms of Si and Pt tips, we conclude that the Pt tip is stiffer than the Si tip.

The depth of the energy dip is shallower than that of the Si tip case with the same tip-surface distance. This is due to the difference between the Si-Ag and Pt-Ag bonds, and the sharpness and the stiffness of the tip apex structure. As mentioned above, the Pt tip apex atom does not move toward the Ag atom. Therefore the bond length of the tip apex atom and the Ag atom bond stays longer than that of the Si tip. Moreover, as plotted in Fig. 6(b), the energy gain by the formation of the Pt-Ag bond is about 1.0 eV at most which is much smaller than that of the 1.6 eV of the Si-Ag bond. The considered Pt tip is sharper than the Si tip. Even at the 3.5 Å tip-surface distance, the Ag atom is interacting with the tip mostly by the tip apex Pt atom unlike the Si tip case (see Fig. 8). But with the smaller tip-surface distance, it is expected that the Ag atom would interact strongly with the second layer atom of the tip and the trapping effect would be enhanced.

The energy barrier of the diffusion along *pathway 3* is not reduced by the presence of the tip. As shown in Fig. 6, the interaction between the Ag atom and the Pt tip starts from a closer distance than the interaction between the Ag atom and the Si tip. Thus, even at the tip-surface distance of 3.5 Å, there is no significant interaction between the Ag atom and the Pt tip at the saddle point configuration. Moreover, similar to the gate controlling with the Si tip, the trap potential is shallower in *pathway 3*. Therefore, these results show that the inter-HUC diffusion channel is changed from *pathway 3* to *pathway 1* with the presence of the Pt tip.

Even though less substantial than that by the Si tip, our results show that the diffusion controlling of the Ag atom diffusion between HUC of Si(111) surface is possible with the Pt tip. This is consistent with the experimental situation in which the Pt-Ir coated tip is successfully utilized to control the inter-HUC diffusion [12].

IV. SUMMARY

We have performed total-energy electronic-structure calculations using density functional theory for the diffusion of the Ag atom between the half unit cells (HUCs) on the Si(111)-(7×7) surface with and without the probing tip of the atomic force microscope (AFM). We have first clarified the atom-scale reaction pathways and the corresponding energy barriers for the Ag atom diffusion on the surface. There are three pathways of the inter-HUC diffusion connecting the (meta)stable adsorption sites in the two HUCs. The pathway with the lowest energy barrier passes over the nanohole. In the center of the nanohole, the Ag atom is lowered to the same height as the second layer Si atoms. The energy barrier of the diffusion from unfaulted-HUC (UHUC) to faulted-HUC (FHUC) along this pathway is 0.79 eV. The other two pathways

pass through the edge of the nanohole. In the middle of each of these two pathways, there is a metastable adsorption site rendering the diffusion to be a two-step process. The energy barriers of the rate determining processes in UHUC to FHUC diffusion (forward diffusion) and the reverse diffusion (backward diffusion) along these two pathways are about 1 eV. We have also identified the reaction pathways and the corresponding energy barriers for the diffusion with the presence of the Si and Pt tips of the AFM. When the tip is placed slightly off to the side of the FHUC from the boundary of the HUCs, the energy barriers of the forward and the backward diffusions become asymmetric. We have found that the diffusion channel changes from the pathway that passes over the nanohole to the other two pathways with the presence of the AFM tip. This is due to the large distance between the Ag atom and the tip apex atom in this pathway compared to the other two pathways. For the pathways along the edge of the surface nanohole, the energy barriers of the intended diffusion (forward diffusion) decrease with the small tip-surface distance. The Si tip reduces the barrier more substantially than the Pt tip. We have found that the flexibility of the tip apex structure was crucial in the drastic lowering of the energy barrier. In addition to the barrier lowering effect, the tip traps the adatom near the tip apex, preventing backward diffusion to take place. The energy barrier of backward diffusion stays larger than 1 eV for any tip-surface distance. The trapping effect of the tip is enhanced by the interaction between the diffusing adatom and the second layer atom of the tip. The bond formation between the AFM tip atom and the surface adatom is the essential physics for the atom manipulation. Our calculations show that diffusion controlling is possible with both metallic and semiconducting AFM tips.

ACKNOWLEDGMENTS

This work was supported by Ministry of Education, Culture, Sports, Science and Technology as a social and scientific priority issue (creation of new functional devices and high-performance materials to support next-generation industries) to be tackled by using post-K computer. Computations were performed mainly at the Supercomputer Center at the Institute for Solid State Physics, The University of Tokyo, The Research Center for Computational Science, National Institutes of Natural Sciences, and the Center for Computational Science, University of Tsukuba.

[1] G. Binnig, H. Rohrer, C. Gerber, and E. Weibel, Phys. Rev. Lett. **49**, 57 (1982).
[2] G. Binnig, C. F. Quate, and C. Gerber, Phys. Rev. Lett. **56**, 930 (1986).
[3] D. M. Eigler and E. K. Schweizer, Nature (London) **344**, 524 (1990).
[4] I.-W. Lyo and P. Avouris, Science **253**, 173 (1991).
[5] N. Oyabu, O. Custance, I. Yi, Y. Sugawara, and S. Morita, Phys. Rev. Lett. **90**, 176102 (2003).
[6] Y. Sugimoto, P. Pou, O. Custance, P. Jelinek, M. Abe, R. Pérez, and S. Morita, Science **322**, 413 (2008).
[7] Y. Sugimoto, M. Abe, S. Hirayama, N. Oyabu, O. Custance, and S. Morita, Nat. Mater. **4**, 156 (2005).
[8] Y. Sugimoto, O. Custance, M. Abe, and S. Morita, e-J. Surf. Sci. Nanotech. **4**, 376 (2006).
[9] Y. Sugimoto, P. Jelinek, P. Pou, M. Abe, S. Morita, R. Perez, and O. Custance, Phys. Rev. Lett. **98**, 106104 (2007).
[10] Y. Sugimoto, A. Yurtsever, M. Abe, S. Morita, M. Ondráček, P. Pout, R. Pérez, and P. Jelinek, ACS Nano **7**, 7370 (2013), and references therein.
[11] N. Oyabu, Y. Sugimoto, M. Abe, O. Custance, and S. Morita, Nanotechnology **16**, S112 (2005).
[12] Y. Sugimoto, A. Yurtsever, N. Hirayama, M. Abe, and S. Morita, Nat. Commun. **5**, 4360 (2014).
[13] M. S. Ho, C. C. Su, and T. T. Tsong, Jpn. J. Appl. Phys. **45**, 2382 (2006).
[14] P. Sobotík, P. Kocán, and I. Ošt'ádal, Surf. Sci. **537**, L442 (2003).
[15] Y. Sugimoto, Y. Nakajima, D. Sawada, K. I. Morita, M. Abe, and S. Morita, Phys. Rev. B **81**, 245322 (2010).
[16] L. Pizzagalli and A. Baratoff, Phys. Rev. B **68**, 115427 (2003).
[17] T. Trevethan, L. Kantorovich, J. Polesel-Maris, S. Gauthier, and A. Shluger, Phys. Rev. B **76**, 085414 (2007).
[18] M. Haruta, N. Yamada, T. Kobayashi, and S. Iijima, J. Catal. **115**, 301 (1989).
[19] M. Haruta, Catal. Today **36**, 153 (1997).
[20] M. Valden, X. Lai, and D. W. Goodman, Science **281**, 1647 (1998).
[21] E. J. Van Leonen, M. Iwanami, R. M. Tromp, and J. F. Van Der Veen, Surf. Sci. **137**, 1 (1984).
[22] St. Tosch and H. Neddermeyer, Phys. Rev. Lett. **61**, 349 (1988).
[23] K. J. Wan, X. F. Lin, and J. Nogami, Phys. Rev. B **47**, 13700 (1993).
[24] H. Hirayama, H. Okamoto, and K. Takayanagi, Phys. Rev. B **60**, 14260 (1999).
[25] P. Sobotík, I. Ošt'ádal, and P. Kocán, Surf. Sci. **604**, 1778 (2010).
[26] F. Ming, K. Wang, X. Zhang, J. Liu, A. Zhao, J. Yang, and X. Xiao, J. Phys. Chem. C **115**, 3847 (2011).
[27] K. Wang, C. Zhang, M. M. T. Loy, and X. Xiao, Phys. Rev. Lett. **94**, 036103 (2005).
[28] F. Ming, K. Wang, S. Pan, J. Liu, X. Zhang, J. Yang, and X. Xiao, ACS Nano **5**, 7608 (2011).
[29] C. Zhang, G. Chen, K. Wang, H. Yang, T. Su, C. T. Chan, M. M. T. Loy, and X. Xiao, Phys. Rev. Lett. **94**, 176104 (2005).
[30] K. Wang, G. Chen, C. Zhang, M. M. T. Loy, and X. Xiao, Phys. Rev. Lett. **101**, 266107 (2008).
[31] P. Hohenberg and W. Kohn, Phys. Rev. **136**, B864 (1964).
[32] W. Kohn and L. J. Sham, Phys. Rev. **140**, A1133 (1965).
[33] G. Kresse and J. Hafner, Phys. Rev. B **47**, 558 (1993).
[34] G. Kresse and J. Furthmüller, Phys. Rev. B **54**, 11169 (1996).
[35] J. P. Perdew, K. Burke, and M. Ernzerhof, Phys. Rev. Lett. **77**, 3865 (1996); **78**, 1396 (1997).
[36] P. E. Blöchl, Phys. Rev. B **50**, 17953 (1994).
[37] G. Kresse and D. Joubert, Phys. Rev. B **59**, 1758 (1999).
[38] B. Enkhtaivan and A. Oshiyama, Phys. Rev. B **94**, 085416 (2016).

[39] K. Takayanagi, Y. Tanishiro, S. Takahashi, and M. Takahashi, Surf. Sci. **164**, 367 (1985).
[40] G. Henkelman, B. P. Uberuaga, and H. Jónsson, J. Chem. Phys. **113**, 9901 (2000).
[41] S. Jeong and A. Oshiyama, Phys. Rev. Lett. **81**, 5366 (1998).
[42] P. Pou, S. A. Ghasemi, P. Jelinek, T. Lenosky, S. Geodecker, and R. Perez, Nanotechnology **20**, 264015 (2009).
[43] R. Pérez, M. C. Payne, I. Štich, and K. Terakura, Phys. Rev. Lett. **78**, 678 (1997).
[44] R. Pérez, I. Štich, M. C. Payne, and K. Terakura, Phys. Rev. B **58**, 10835 (1998).
[45] P. Dieška, I. Štich, and R. Pérez, Phys. Rev. Lett. **91**, 216401 (2003).
[46] S. Jarvis, A. Sweetman, J. Bamidele, L. Kantorovich, and P. Moriarty, Phys. Rev. B **85**, 235305 (2012).
[47] Here we adopt the naming given in the previous works (Europhys. Lett. **39**, 287 (1997); Surf. Sci. **396**, L261 (1998); and Ref. [27]).
[48] When the tip structure is not allowed to relax, the diffusion barrier remains as high as 0.63 eV even when the tip-surface distance is 3.5 Å.